Materials Science & Engineering C 99 (2019) 367–373

Contents lists available at ScienceDirect

Materials Science & Engineering C

journal homepage: www.elsevier.com/locate/msec

The effect of different occlusal contact situations on peri-implant bone stress – A contact finite element analysis of indirect axial loading

Annike Brune, Meike Stiesch, Michael Eisenburger, Andreas Greuling*

Department of Prosthetic Dentistry and Biomedical Materials Science, Hannover Medical School, 30625 Hannover, Germany

ARTICLE INFO

Keywords:
Finite element analysis
Dental implants
Biomedical engineering
Bite force
Dental stress analysis
Dental occlusion

ABSTRACT

Implant restoration is one of the basic treatments in dentistry today, yet implant loss from occlusal overload is still a problem. Complex biomechanical problems such as occlusal overload are often analyzed by means of the finite element method. This numerical method makes it possible to analyze in detail the influence that different loading situations have upon implants and tissues, which is a key element in optimizing these dental procedures.

This study was designed to investigate the stress distribution in peri-implant bone of a single-tooth implant crown using the finite element method. The load was applied indirectly via an occluding tooth through a three and five contact setup into the implant crown. The friction coefficient values between the crown and antagonist were varied between 0.1 and 1.0. Additionally, three crowns with cusp inclinations of 20°, 30° and 40° were modeled. Non-linear contact computations indicated that an increase in friction changed the direction and magnitude of contact forces, which also led to reduced stresses in the bone. Furthermore, the stress magnitudes were higher when cusps of a greater inclination were used. The intensity of stress alterations was strongly dependent on the distribution and number of contacts, and the contact force vector. In maximum intercuspation, a resulting axial load due to well-distributed contacts prevented high stresses in bone even with high cusp inclinations and low friction. Therefore for long-term clinical success, particular attention should be paid to occlusal adjustment so as to prevent oblique loading onto dental implant restorations.

1. Introduction

Implant prosthetic reconstructions are exposed to various biological and biomechanical impacts [1]. Poor oral hygiene can result in peri-implant infections of soft and hard tissue causing bone loss, which can be worsened in situations with poor bone quality or high susceptibility to infections [2,3]. Similarly, high biomechanical loads can cause high mechanical stress in the bone surrounding the implants also resulting in bone loss [4]. Both impacts can be finally responsible for implant loss.

A major topic of dental research in the area of implant loss prevention is the investigation, evaluation and prevention of occlusal overload. In recent years, the finite element analysis (FEA) has commonly been used to investigate the effect of occlusal loads on dental implants and the surrounding bone [5]. By means of this simulation method, physical factors, such as mechanical stress and strain, can be computed and illustrated [6]. However, these types of biomechanical simulations are very challenging, since the material properties of living tissue are highly complex. Nevertheless, simulations have been used successfully to compute stress distributions and create improved treatment procedures that increase the lifespan of dental implants [7].

A crucial factor for implant survival is the distribution, the direction and the size of occlusal forces that act onto the implant, the surrounding bone and the prosthetic reconstruction [8]. In most simulation studies, the occlusal forces are applied directly to the dental restorations [5,9,10]. There are only a few finite element studies that apply the force indirectly via a corresponding antagonist [11,12]. The advantage of this method is that contact phenomena, such as friction and sliding between the contact partners, can also be taken into consideration. By means of a mathematical analysis, Katona [13] demonstrated that a change in the coefficient of friction influences the direction and magnitude of the contact force. The coefficient of friction was strongly influenced by the loading, the surface properties of the contacting surfaces and the environment. Over the past few decades, many studies have been performed to investigate the friction behavior of dental materials (ceramics, alloys, polymers) against the natural tooth enamel or other dental materials in wet or dry environments. It was discovered that the surface

* Corresponding author at: Department of Prosthetic Dentistry and Biomedical Materials Science, Hannover Medical School, Carl-Neuberg-Str. 1, 30625 Hannover, Germany.

E-mail addresses: Brune.Annike@mh-hannover.de (A. Brune), Stiesch.Meike@mh-hannover.de (M. Stiesch), Eisenburger.Michael@mh-hannover.de (M. Eisenburger), Greuling.Andreas@mh-hannover.de (A. Greuling).

https://doi.org/10.1016/j.msec.2019.01.104
Received 28 June 2018; Received in revised form 21 January 2019; Accepted 23 January 2019
Available online 30 January 2019
0928-4931/

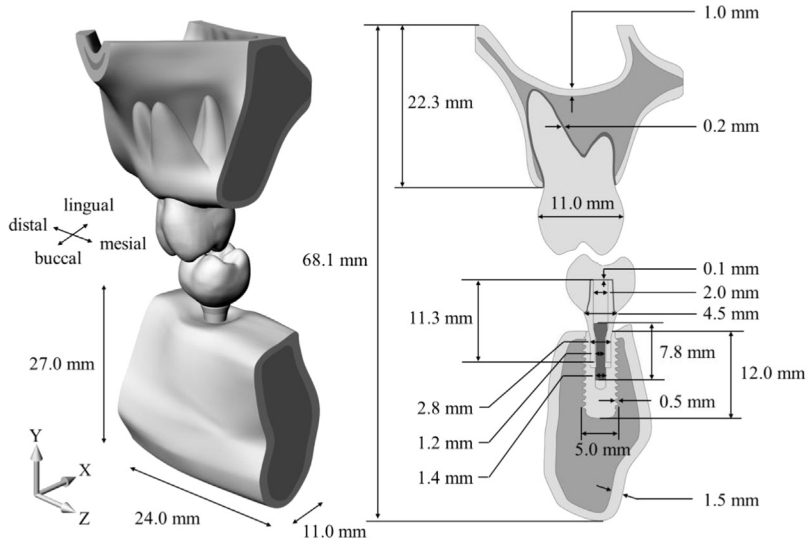

Fig. 1. Configuration of the investigated model: perspective and sectional view: mandibular jaw section, dental implant system, single crown (46), upper first left molar (16), periodontal ligament and maxillary jaw section.

roughness depends on the final finishing quality, fracture toughness, hardness [14], porosities and defects [15], fillers [16] and chemical stability [17] of the contact materials. In addition, saliva's action as a lubricant also affects the coefficient of friction. This lubricant effect becomes more or less pronounced depending upon the patient's age, diet, disease and medications [13,18,19].

The aim of the current study is to investigate the influence of contact area arrangement, cusp inclination and friction coefficient between an antagonist and the implant crown upon the maximum and minimum principal stresses in peri-implant bone. The contact simulation method and models used in this study are nearly identical to those used in a previous work by Rand et al. [12].

2. Materials and methods

2.1. Geometry acquisition

A three dimensional NURBS model (Non-Uniform Rational B-Spline) (Fig. 1) was generated using the software Rhinoceros 5.0 (McNeel North America, Seattle, WA, USA). The lower part of the model consists of a left mandibular jaw section (molar region) and a generic dental implant system (implant, abutment, screw) with a cemented single crown. The upper part of the model consists of a left maxillary jaw section (molar region), retaining an upper first left molar (antagonist) and its periodontal ligament. More detailed information about the 3D dental model can be found in the prior work of Rand et al. [12]. In the current study a new upper jaw section and a monolithic full ceramic crown were added, with the full ceramic crown being used to replace the veneered framework from the previous model. The upper jaw section consists of cancellous bone surrounded by a layer of cortical bone, as does the lower jaw section.

The implant crown and its antagonist were positioned in Angle Class I occlusion. This is equivalent to the position of the antagonist and crown in the previous work. The occlusal surfaces of antagonist and crown were modified to get maximum intercuspation with three and five occlusal contact areas (CAs) (Fig. 2b). To evaluate the influence of occlusal cusp inclination the crown was modeled with cusp inclinations of 20° (flat), 30° (medium) and 40° (steep) (± 2.5°) in the contact areas (Fig. 2a).

2.2. Material, contact and meshing properties

The 3D NURBS models were imported into ANSYS Workbench 18.0 (Swanson Analysis, Huston, PA, USA). The material properties of all parts were considered as homogeneous and isotropic in the analyses. The elastic modulus for abutment, implant and screw (titan) was defined as 110,000 MPa with a Poisson's ratio of 0.35 [20]. The monolithic zirconia crown (3Y-TZP) had an elastic modulus of 210,000 MPa and a Poisson's ratio of 0.27 [21]. The Elastic modulus for cortical bone was set to 13,700 MPa and the modulus of cancellous bone to 1370 MPa, with a Poisson's ratio of 0.3 [22]. An elastic modulus of 68.9 MPa and Poisson's ratio of 0.45 were assigned to the periodontal ligament [23]. For the antagonist an average elastic modulus of 18,600 MPa was assumed for the simulation, with a Poisson's ratio of 0.31 [24]. The cement layer (glass ionomer cement) was taken to have an elastic modulus of 15,900 MPa and a Poisson's ratio of 0.33 [25].

The contact between the occlusal surfaces of the antagonist and the crown was defined as frictional. The friction coefficient values were varied between 0.1 and 1.0 in increments of 0.1. All other contact surfaces of the different parts were bonded by forming a multibody part. The detailed explanation for this approach and the settings used can be found in Rand et al. [12]. In this previous work a convergence test was used to check the accuracy of the model. Particular attention was paid to the peri-implant region of the lower cortical and cancellous bone. The evaluation revealed that a singularity occurred in the area of interest. The same insights were found by Petrie and Williams [26]. Nevertheless, it is reasonable to compare the stress results obtained from the models used in this and the previous study, since the same mesh was used in the region where the singularity occurred. However, the absolute stress values might be questionable in the setting of a singularity.

2.3. Load and boundary conditions

The mandibular jaw section was moved parallel to the implant axis towards the maxillary jaw section, until an initial contact between crown and antagonist arose. Then a force of 100 N was applied in the same axial direction, up through the base of the mandibular jaw section (checkered face in Fig. 3). Any transverse translations of the mandibular jaw section base were prevented. The lateral intersections (striped faces in Fig. 3) of the upper cortical and cancellous bone were

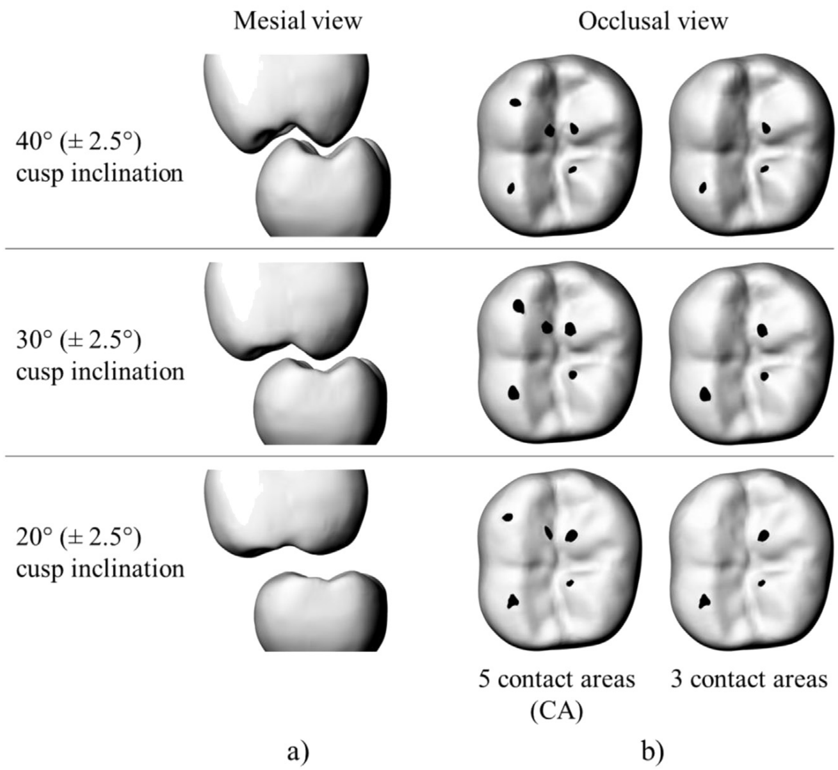

Fig. 2. Configuration of the crown-to-tooth occlusion: a) crown and antagonist with 40°, 30° and 20° cusp inclinations in the area of contacts, b) resulting CAs on tooth 46 for two contact situations (three and five CAs).

set as frictionless. This means that no portion of the intersection faces could move, rotate, or deform normal to the face. The upper intersection of the upper cortical bone was fixed horizontally and vertically (black faces in Fig. 3).

2.4. Evaluation of results

The compression and tensile stress values (maximum and minimum principal stress) in the peri-implant region of the cortical and cancellous bone (mandibular jaw section) were used to evaluate the influence of different load situations. Principal stresses are appropriate measures for brittle materials such as bone and are frequently used in biomechanical FE studies [27–29]. In addition, the total contact force reaction and its components in the X- and Z-directions (Y = 100 N) were computed to analyze the displacement of the implant and the effects upon bone stress.

3. Results

Figs. 4 and 5 show the stress distributions (maximum and minimum

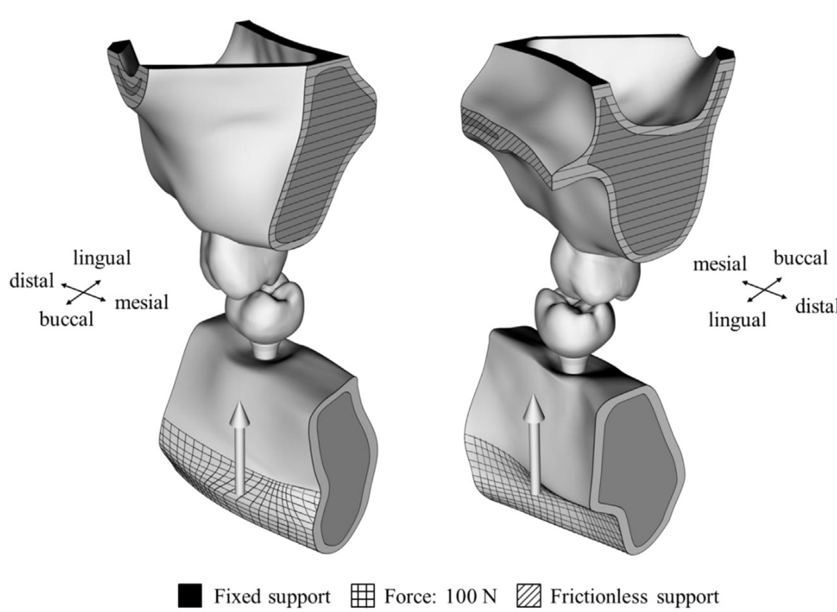

Fig. 3. Boundary conditions and applied loading (arrow) for the used model from two different views: mesial/buccal (left) and distal/lingual (right).

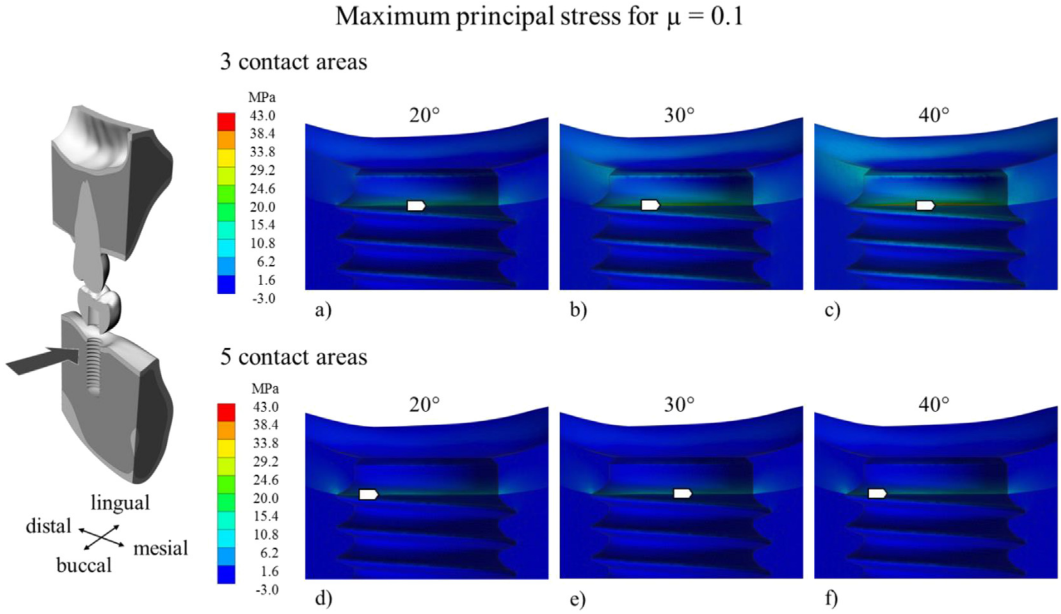

Fig. 4. Distribution of maximum principal stresses in peri-implant bone with a friction coefficient of μ = 0.1. The broad arrow indicates the direction of view for images a) to f). a) 3 contacts and 20° cusp inclination, b) 3 contacts and 30° cusp inclination, c) 3 contacts and 40° cusp inclination, d) 5 contacts and 20° cusp inclination, e) 5 contacts and 30° cusp inclination and f) 5 contacts and 40° cusp inclination.

principal stress) for a friction coefficient of μ = 0.1 in the cortical and cancellous bone near the implant neck on the lingual side of the mandibular jaw section. The position of the highest maximum and lowest minimum principal stress values are indicated by white flags. In both contact situations (three and five CAs) with all three cusp inclinations (20°, 30° and 40°), the highest stresses were concentrated in the cortical bone, directly at the border of the cancellous bone. The highest maximum principal stress values in the implant-bone interface occurred with maximum intercuspation, and their values were: a) 19.9 MPa for three CAs on flat cusps, b) 32.4 MPa for three CAs on medium cusps, c) 42.1 MPa for three CAs on steep cusps, d) 12.1 MPa for five CAs on flat cusps, e) 12.4 MPa for five CAs on medium cusps and f) 13.6 MPa for five CAs on steep cusps (Fig. 4).

The lowest stresses were concentrated in the cortical crest, again in both contact situations for all three cusp inclinations. The lowest minimum principal stress values were: a) −22.7 MPa for three CAs on flat cusps, b) −36.5 MPa for three CAs on medium cusps, c) −49.2 MPa for three CAs on steep cusps, d) −10.9 MPa for five CAs on flat cusps, e) −13.0 MPa for five CAs on medium cusps and f) −12.9 MPa for five CAs on steep cusps (Fig. 5).

Fig. 6 shows the lowest minimum and highest maximum principal stress values in the cortical bone for each test scenario. The results for the "3CAs" groups demonstrate that when the friction is higher, the stress magnitudes are smaller in the cortical bone – with both the

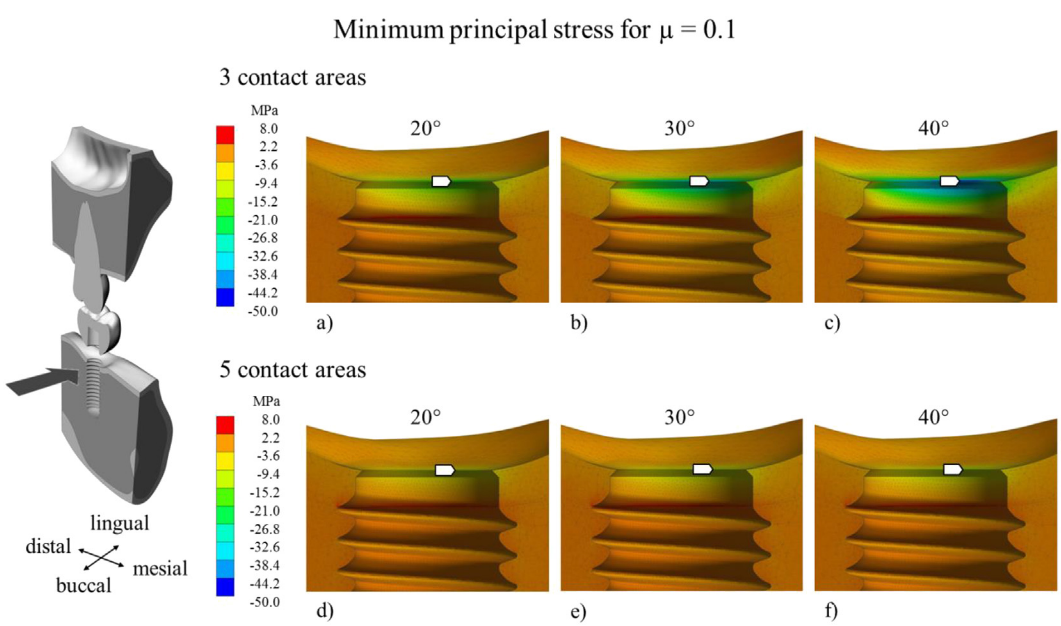

Fig. 5. Distribution of minimum principal stresses in peri-implant bone with a friction coefficient of μ = 0.1. The broad arrow indicates the direction of view for images a) to f). a) 3 contacts and 20° cusp inclination, b) 3 contacts and 30° cusp inclination, c) 3 contacts and 40° cusp inclination, d) 5 contacts and 20° cusp inclination, e) 5 contacts and 30° cusp inclination and f) 5 contacts and 40° cusp inclination.

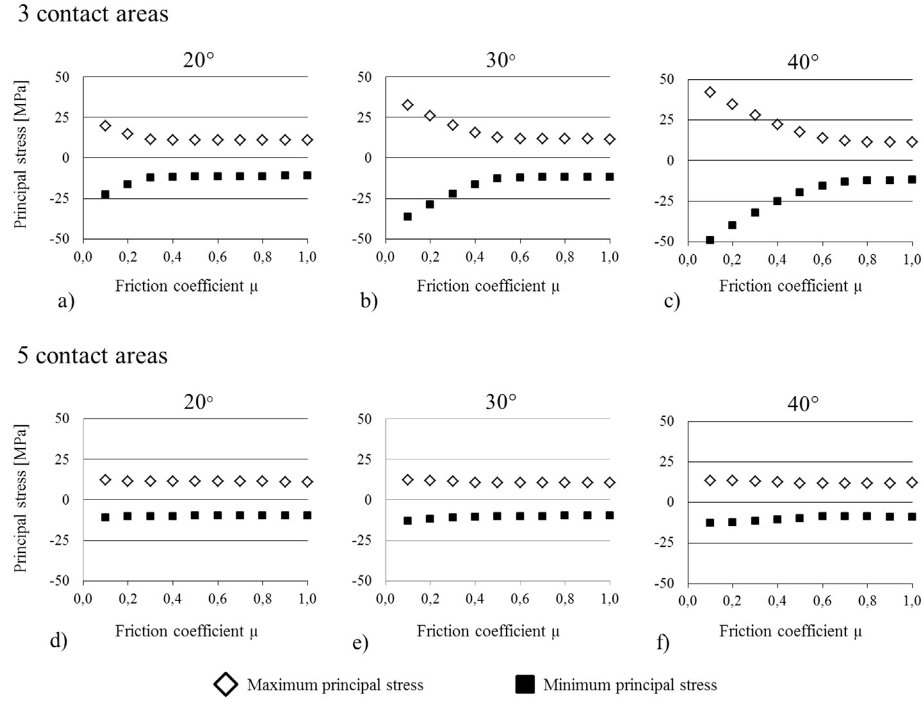

Fig. 6. The lowest minimum and highest maximum principal stress values in the cortical bone for three and five contact areas with cusp inclinations of 20°, 30° and 40°, and friction coefficient values between 0.1 and 1.0.

tensile and compressive stresses for all three groups approaching the respective values of 12 MPa and −12 MPa at higher coefficients of friction. Only slight differences in the magnitudes can be observed between the three groups with five CAs. Additionally, major differences were noted between the various inclination groups with three CAs. Firstly, average stress values increased with increasing cusp inclination. Secondly, although all 3 group's magnitudes decreased towards the same tensile and compressive stresses, the rate of reduction flattened out to less than 2% at a higher coefficient of friction with the steeper cusps (friction values respectively of 0.4, 0.6 and 0.8 for inclinations of 20°, 30° and 40°). The stress values in group "5CA/40°" did not decrease steadily, and their tensile and compressive stresses were the lowest at friction coefficient values of 0.6 and 0.7, respectively.

Fig. 7 shows the total contact force reaction and its X-/Z-magnitudes as a function of the friction coefficients. The vector direction and magnitude of contact force reaction in the groups "5CA/20°", "5CA/30°" and "5CA/40°" varied only slightly with friction coefficients ranging from 0.1 to 1.0. Whereas for groups "3CA/20°", "3CA/30°" and "3CA/40°" the magnitude of the contact force reaction decreased with increasing coefficients of friction. This applied particularly to the X-magnitude, which points in a lingual direction.

4. Discussion

In the present study, the highest tensile and compressive stress values occurred in the cortical bone of the upper bone-implant interface and never in the cancellous bone. This is in agreement with several other studies which also investigated the influence of occlusal load on the implant-bone interface by finite element analysis [30–32]. The cortical bone with the higher Young's modulus reacts as a fulcrum under oblique load and absorbs higher load than the cancellous bone [31]. The simulations in this study confirm that occlusal overload primarily affects regions around the implant neck. Furthermore, the current study's numerical results suggest that both the risk of occlusal overload and crown stress-distribution performance can be improved by avoiding cusps with steep inclinations – this minimizes oblique loading and hence reduces stress – especially in the setting of cusps that have a non-uniform distribution of the contact surfaces. Bedi et al. [33] reported that cusp inclination reduction may be helpful in preventing high stress values in the crestal bone around the implant and that poor quality bone tends to be affected more. Similar results have been described in the studies by Rungsiyakull et al. [34] and Liu et al. [35].

Each of the individual contacts of the 3 CA situation was chosen deliberately in order to prove if their inadequate distribution causes non-axial contact forces. The three contacts were located on inclined surfaces which were oriented towards the buccal side. Consequently, the crown and the upper part of the implant were pushed in a lingual direction. Thus, the highest stress values occurred on the lingual side of the peri-implant bone. With regards to the contact situation with five CAs, four contacts were on surfaces inclined towards the buccal side and one contact on a surface inclined towards the lingual side. This lingual contact area led to an approximately axial reaction force and to low stress values in the implant-bone interface. Eskitascioglu et al. [36] results also demonstrated the significant influence that the number and location of occlusal loading areas has upon stress distributions. Carlsson [37] gave some general guidelines for therapeutic occlusion, where he recommended using well-distributed contacts in maximum intercuspation in order to achieve axially directed forces. In addition, a previous study of Rand et al. [12] illustrated the influence of occlusal contact area and number on the peri-implant bone stresses. Further simulations are planned for the future, in which new FE models with different occlusal contact situations will be investigated. This should make it possible to discuss special features and individual differences in order to get a better understanding of the behavior in different contact situations.

Similarly, lateral movement of the lower jaw is only relevant when canine guidance is absent. In this scenario the only contact during jaw movements is on the buccal cusps resulting in a non-axial directed force. This situation is similar to that of the three contact situation in the current study, since all of their CAs are located on the buccal side of the cusp slopes. Nevertheless, further simulations might be helpful to address more precisely the effects of laterotrusion on the stress distribution in the peri-implant bone.

As mentioned in the introduction, the range of the friction

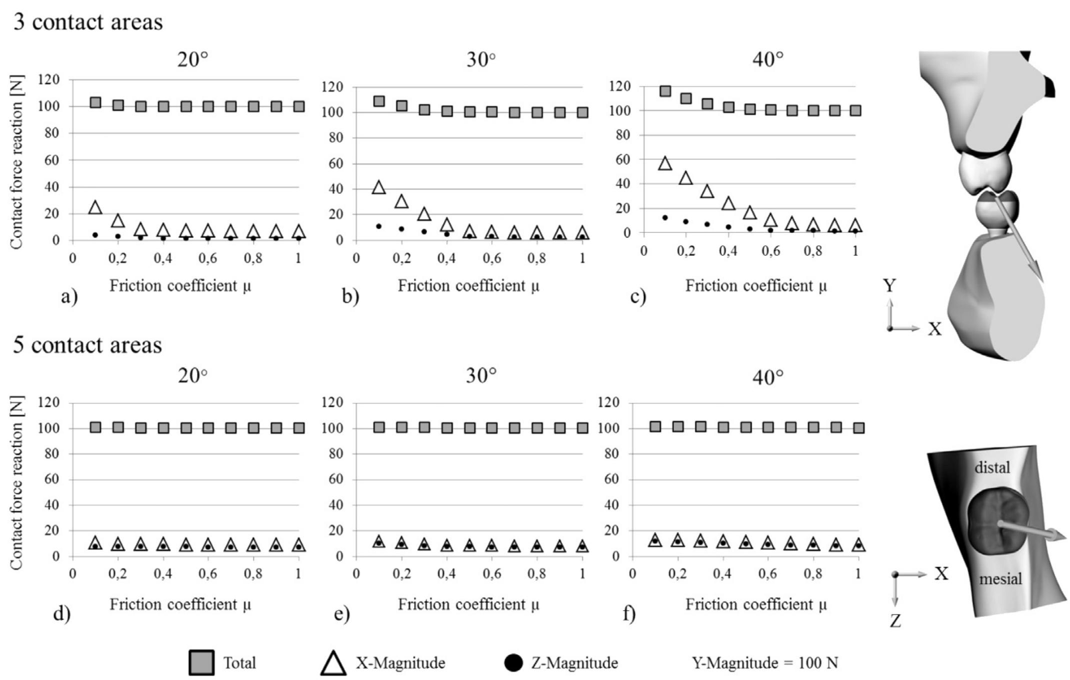

Fig. 7. Total and X-/Z-magnitude of contact force reaction as a function of friction coefficients for three and five CAs, each with cusp inclinations set at 20°, 30° and 40°. The Y-magnitude is equal to 100 N and is not displayed.

coefficient factor is very high in dentistry because of different influencing factors [13–19]. Hence, a linearly increasing parameter series with 10 coefficients of friction was used (0.1–1.0) to determine their effect on maximum and minimum stress distribution in cortical and cancellous bone. In the case of five CAs, all of the friction coefficient values only had a slight effect upon the stress magnitude, because the distribution of the CAs inherently minimizes non-axial components of the force. However, when considering the non-axial load situation with three CAs, a high coefficient of friction helps to avoid high stresses in peri-implant bone. A dry environment with, clinically more realistic, rough contact surfaces would cause high friction and therefore help reduce any peri-implant stress. Unfortunately these conditions also promote plaque formation [38] and/or facilitate wear of the antagonist [17,39]. Thus, the friction coefficient should neither be too low because of the resultant oblique loading, nor be too high due to the associated potential for greater wear and plaque formation. Zheng and Zhou [40] studied the effect that age has upon the friction and wear behaviors of human teeth. They found that the wear-resistance decreases and the surface roughness increases with age. Hence when considering this in context of the current study's findings, the normal wear behavior of human teeth over time leads to a natural reduction in stress in peri-implant bone tissue.

The current finite element study has some limitations. Maxillary and mandibular jaw sections, tooth and periodontal ligament were all considered isotropic, homogeneous and linearly elastic. Furthermore, the abutment screw had no threads and the contact surfaces between screw, abutment and implant were firmly connected. The main reason for these simplifications was to reduce computation times.

Previous work by the same authors revealed that infinitely high loads (singularity) occurred in the peri-implant region of the lower cortical bone after performing a convergence check. The singularity occurs because of the Young's modulus differences between implant, cancellous and cortical bone, and the presence of sharp corners on the cortical bone. The effect of different load conditions on a jaw section with an implant-supported crown is often examined by means of the finite element method, yet the existence of a stress singularity in the cortical bone is rarely mentioned in discussions. One should bear in mind that the maximum stress value close to the singularity strongly depends on the size of the mesh.

5. Conclusion

Within the limitations of this three-dimensional finite element study, the following conclusions can be drawn:

- In all of the contact situations that were examined, the highest maximum and lowest minimum principal stresses were always located in the cortical bone and never in the cancellous bone which is consistent with the existing literature.
- The coefficient of friction between crown and its occluding tooth influenced the direction and magnitude of the resulting contact force. The peri-implant bone stress decreased with increasing coefficient friction. With respect to a minimization of peri-implant bone stress, a high friction between crown and antagonist seems favorable. However, a roughening of the occlusal surface has the drawback of inferior surface quality leading to a lower crack resistance and a higher adherence of dental plaque.
- In the case of non-uniform contact distribution (three CAs) the stress in the implant-bone interface increased with increasing cusp inclination, whereas in the setting of well-distributed contacts the cusp inclination failed to demonstrate a meaningful influence on peri-implant bone stress.
- Badly distributed contacts in maximum intercuspation should generally be avoided, because they cause non-axial forces which lead to high peri-implant bone stresses.

Declarations of interest

None.

Acknowledgments

We thank Dr. Timothy Price for critical reading and editing of the manuscript.

References

[1] T.-J. Oh, J. Yoon, C.E. Misch, H.-L. Wang, The causes of early implant bone loss: myth or science? J. Periodontol. 73 (2002) 322–333, https://doi.org/10.1902/jop.2002.73.3.322.
[2] K. Heydenrijk, H.J. Meijer, W.A. van der Reijden, G.M. Raghoebar, A. Vissink, B. Stegenga, Microbiota around root-form endosseous implants: a review of the literature, Int. J. Oral Maxillofac. Implants 17 (2002).
[3] L.W. Lindquist, B. Rockler, G.E. Carlsson, Bone resorption around fixtures in edentulous patients treated with mandibular fixed tissue-integrated prostheses, J. Prosthet. Dent. 59 (1988) 59–63, https://doi.org/10.1016/0022-3913(88)90109-6.
[4] C.E. Misch, J.B. Suzuki, F.M. Misch-Dietsh, M.W. Bidez, A positive correlation between occlusal trauma and peri-implant bone loss: literature support, Implant. Dent. 14 (2005) 108–116, https://doi.org/10.1097/01.id.0000165033.34294.db.
[5] S. Trivedi, Finite element analysis: a boon to dentistry, J. Oral Biol. Craniofac. Res. 4 (2014) 200–203, https://doi.org/10.1016/j.jobcr.2014.11.008.
[6] A. Srirekha, K. Bashetty, Infinite to finite: an overview of finite element analysis, Indian J. Dent. Res. 21 (2010) 425–432, https://doi.org/10.4103/0970-9290.70813.
[7] M.-L. Hsu, C.-L. Chang, Application of finite element analysis in dentistry, in: D. Moratal (Ed.), Finite Element Analysis, IntechOpen, Rijeka, 2010, pp. 43–60.
[8] R.A. Sheridan, A.M. Decker, A.B. Plonka, H.-L. Wang, The role of occlusion in implant therapy: a comprehensive updated review, Implant. Dent. 25 (2016) 829–838, https://doi.org/10.1097/ID.0000000000000488.
[9] C. Costa, N. Peixinho, J.P. Silva, S. Carvalho, Study and characterization of the crest module design: a 3D finite element analysis, J. Prosthet. Dent. 113 (2015) 541–547, https://doi.org/10.1016/j.prosdent.2014.12.008.
[10] A. Rand, P. Kohorst, A. Greuling, L. Borchers, M. Stiesch, Stress distribution in all-ceramic posterior 4-unit fixed dental prostheses supported in different ways: finite element analysis, Implant. Dent. 25 (2016) 485–491, https://doi.org/10.1097/ID.0000000000000429.
[11] S. Benazzi, H.N. Nguyen, O. Kullmer, K. Kupczik, Dynamic modelling of tooth deformation using occlusal kinematics and finite element analysis, PLoS ONE 11 (2016) 1–17, https://doi.org/10.1371/journal.pone.0152663.
[12] A. Rand, M. Stiesch, M. Eisenburger, A. Greuling, The effect of direct and indirect force transmission on peri-implant bone stress—a contact finite element analysis, Comput. Methods Biomech. Biomed. Engin. 20 (2017) 1132–1139, https://doi.org/10.1080/10255842.2017.1338691.
[13] T.R. Katona, A mathematical analysis of the role of friction in occlusal trauma, J. Prosthet. Dent. 86 (2001) 636–643, https://doi.org/10.1067/mpr.2001.120068.
[14] E. Tillitson, R. Craig, F. Peyton, Friction and wear of restorative dental materials, J. Dent. Res. 50 (1971) 149–154.
[15] K.D. Jørgensen, Restorative resins: abrasion vs. mechanical properties, Eur. J. Oral Sci. 88 (1980) 557–568, https://doi.org/10.1111/j.1600-0722.1980.tb01267.x.
[16] Y. Zhang, D. Xu, P. Rao, M. Lü, J. Wu, Friction behavior of dental porcelain with different leucite particle sizes, J. Am. Ceram. Soc. 91 (2008) 1678–1681, https://doi.org/10.1111/j.1551-2916.2008.02312.x.
[17] W.-s. Oh, R. DeLong, K.J. Anusavice, Factors affecting enamel and ceramic wear: a literature review, J. Prosthet. Dent. 87 (2002) 451–459, https://doi.org/10.1067/mpr.2002.123851.
[18] W. Douglas, R. Sakaguchi, R. DeLong, Frictional effects between natural teeth in an artificial mouth, Dent. Mater. 1 (1985) 115–119, https://doi.org/10.1016/S0109-5641(85)80040-3.
[19] A. Koran, R. Craig, E. Tillitson, Coefficient of friction of prosthetic tooth materials, J. Prosthet. Dent. 27 (1972) 269–274, https://doi.org/10.1016/0022-3913(72)90034-0.
[20] J. Yang, H.J. Xiang, A three-dimensional finite element study on the biomechanical behavior of an FGBM dental implant in surrounding bone, J. Biomech. 40 (2007) 2377–2385, https://doi.org/10.1016/j.jbiomech.2006.11.019.
[21] C. Piconi, G. Maccauro, Zirconia as a ceramic biomaterial, Biomaterials 20 (1999) 1–25, https://doi.org/10.1016/S0142-9612(98)00010-6.
[22] C.-C. Ko, C.-S. Chu, K.-H. Chung, M.-C. Lee, Effects of posts on dentin stress distribution in pulpless teeth, J. Prosthet. Dent. 68 (1992) 421–427, https://doi.org/10.1016/0022-3913(92)90404-X.
[23] A. Weinstein, J. Klawitter, S. Cook, Implant-bone interface characteristics of bioglass dental implants, J. Biomed. Mater. Res. 14 (1980) 23–29, https://doi.org/10.1002/jbm.820140104.
[24] M.-H. Ho, S.-y. Lee, H.-H. Chen, M.-C. Lee, Three-dimensional finite element analysis of the effects of posts on stress distribution in dentin, J. Prosthet. Dent. 72 (1994) 367–372, https://doi.org/10.1016/0022-3913(94)90555-X.
[25] L.A. Denisova, R.G. Maev, I.Y. Poyurovskaya, T.V. Grineva, A.F. Denisov, E.Y. Maeva, E.Y. Bakulin, The use of acoustic microscopy to study the mechanical properties of glass-ionomer cement, Dent. Mater. 20 (2004) 358–363, https://doi.org/10.1016/S0109-5641(03)00129-5.
[26] C.S. Petrie, J.L. Williams, Comparative evaluation of implant designs: influence of diameter, length, and taper on strains in the alveolar crest, Clin. Oral Implants Res. 16 (2005) 486–494, https://doi.org/10.1111/j.1600-0501.2005.01132.x.
[27] L.B. Torcato, E.P. Pellizzer, F.R. Verri, R.M. Falcón-Antenucci, V.E.d.S. Batista, L.F.d.T.P. Lopes, Effect of the parafunctional occlusal loading and crown height on stress distribution, Braz. Dent. J. 25 (2014) 554–560, https://doi.org/10.1590/0103-6440201300144.
[28] F.R. Verri, J.F.S. Junior, D.A. de Faria Almeida, G.B.B. de Oliveira, V.E. de Souza Batista, H.M. Honório, P.Y. Noritomi, E.P. Pellizzer, Biomechanical influence of crown-to-implant ratio on stress distribution over internal hexagon short implant: 3-D finite element analysis with statistical test, J. Biomech. 48 (2015) 138–145, https://doi.org/10.1016/j.jbiomech.2014.10.021.
[29] Y. Yamanishi, S. Yamaguchi, S. Imazato, T. Nakano, H. Yatani, Influences of implant neck design and implant-abutment joint type on peri-implant bone stress and abutment micromovement: three-dimensional finite element analysis, Dent. Mater. 28 (2012) 1126–1133, https://doi.org/10.1016/j.dental.2012.07.160.
[30] L. Baggi, I. Cappelloni, M. Di Girolamo, F. Maceri, G. Vairo, The influence of implant diameter and length on stress distribution of osseointegrated implants related to crestal bone geometry: a three-dimensional finite element analysis, J. Prosthet. Dent. 100 (2008) 422–431, https://doi.org/10.1016/S0022-3913(08)60259-0.
[31] J.F. Santiago, E.P. Pellizzer, F.R. Verri, P.S.P. de Carvalho, Stress analysis in bone tissue around single implants with different diameters and veneering materials: a 3-D finite element study, Mater. Sci. Eng. C Mater. Biol. Appl. 33 (2013) 4700–4714, https://doi.org/10.1016/j.msec.2013.07.027.
[32] G. Vairo, G. Sannino, Comparative evaluation of osseointegrated dental implants based on platform-switching concept: influence of diameter, length, thread shape, and in-bone positioning depth on stress-based performance, Comput. Math. Methods Med. 2013 (2013) 1–15, https://doi.org/10.1155/2013/250929.
[33] S. Bedi, R. Thomas, R. Shah, D.S. Mehta, The effect of cuspal inclination on stress distribution and implant displacement in different bone qualities for a single tooth implant: a finite element study, Int. J. Oral Health Sci. 5 (2015) 80–86, https://doi.org/10.4103/2231-6027.178496.
[34] C. Rungsiyakull, P. Rungsiyakull, Q. Li, W. Li, M. Swain, Effects of occlusal inclination and loading on mandibular bone remodeling: a finite element study, Int. J. Oral Maxillofac. Implants 26 (2011) 527–537.
[35] S. Liu, Y. Liu, J. Xu, Q. Rong, S. Pan, Influence of occlusal contact and cusp inclination on the biomechanical character of a maxillary premolar: a finite element analysis, J. Prosthet. Dent. 112 (2014) 1238–1245, https://doi.org/10.1016/j.prosdent.2014.04.011.
[36] G. Eskitascioglu, A. Usumez, M. Sevimay, E. Soykan, E. Unsal, The influence of occlusal loading location on stresses transferred to implant-supported prostheses and supporting bone: a three-dimensional finite element study, J. Prosthet. Dent. 91 (2004) 144–150, https://doi.org/10.1016/j.prosdent.2003.10.018.
[37] G.E. Carlsson, Dental occlusion: modern concepts and their application in implant prosthodontics, Odontology 97 (2009) 8–17, https://doi.org/10.1007/s10266-008-0096-x.
[38] C.M. Bollenl, P. Lambrechts, M. Quirynen, Comparison of surface roughness of oral hard materials to the threshold surface roughness for bacterial plaque retention: a review of the literature, Dent. Mater. 13 (1997) 258–269, https://doi.org/10.1016/S0109-5641(97)80038-3.
[39] S.P. Passos, Y. Torrealba, P. Major, B. Linke, C. Flores-Mir, J.A. Nychka, In vitro wear behavior of zirconia opposing enamel: a systematic review, J. Prosthodont. 23 (2014) 593–601, https://doi.org/10.1111/jopr.12167.
[40] J. Zheng, Z. Zhou, Effect of age on the friction and wear behaviors of human teeth, Tribol. Int. 39 (2006) 266–273, https://doi.org/10.1016/j.triboint.2004.09.004.